

# Magnetic Circular Dichroism Spectroscopic Studies on the Stereochemistry and Coordination Behavior of Nickel Porphyrins

Sunhee Choi,\*† James A. Phillips,† William Ware, Jr.,† Carol Wittschieben,†  
Craig J. Medforth,‡ and Kevin M. Smith‡

Department of Chemistry and Biochemistry, Middlebury College, Middlebury, Vermont 05753, and  
Department of Chemistry, University of California, Davis, California 95616

Received August 10, 1993\*

The electronic structures and the ligand affinities of several nickel porphyrins with different types and degrees of macrocycle deformations have been studied by magnetic circular dichroism (MCD) spectroscopy. The nickel porphyrins studied in this work are nickel(II) octaethylporphyrin (NiOEP) with a mixture of planar and ruffled porphyrin ring conformations, nickel(II) tetracyclopentenyltetrapentylporphyrin (NiTC<sub>5</sub>TC<sub>5</sub>P) with a ruffled macrocycle, nickel(II) octaethyltetraphenylporphyrin (NiOETPP) with a saddle-shaped macrocycle, and nickel(II) protoporphyrin IX (NiPP) reconstituted hemoglobin (NiHb) and myoglobin (NiMb). The MCD spectra of all three compounds, NiOEP, NiTC<sub>5</sub>TC<sub>5</sub>P, and NiOETPP, consist of mainly normal *A*-term peaks. This indicates that neither the ruffled nor the saddle-shaped conformation lifts the excited state degeneracies, and the *D*<sub>2d</sub> symmetry in both cases is retained. The MCD spectra of NiHb and NiMb consist of normal *A*-term peaks, showing no protein effect on the electronic energy level of nickel porphyrin. There seems to be a correlation between the coordination states of various nickel porphyrins studied in this work and the relative intensity of the Soret MCD band (*I*<sub>S</sub>) to the Q MCD band (*I*<sub>Q</sub>), *I*<sub>S</sub>/*I*<sub>Q</sub>. *I*<sub>S</sub>/*I*<sub>Q</sub> is less than 0.5 for 4-coordinate, approximately 1 for 5-coordinate, and greater than 1.5 for 6-coordinate Ni(II) species. *I*<sub>S</sub>/*I*<sub>Q</sub> of NiTC<sub>5</sub>TC<sub>5</sub>P in pyrrolidine below 100 K is about 3.3, suggesting that pyrrolidine biaxially binds to NiTC<sub>5</sub>TC<sub>5</sub>P. No evidence for axial ligation of pyrrolidine to NiOETPP has been detected down to 2 K. The affinity of NiPP in NiHb or NiMb for exogenous ligands such as 1-methylimidazole, cyanide, azide, and fluoride has been monitored by MCD. None of these ligands bind to NiPP in NiHb or NiMb down to 2 K.

## Introduction

Porphyrins and related tetrapyrroles are of vital importance in biological systems,<sup>1</sup> and there are many industrial applications of the biomimetic chemistries.<sup>2</sup> The tetrapyrrole macrocycle is conformationally flexible and capable of adopting nonplanar conformations.<sup>3</sup> Nonplanar distortions of the tetrapyrrole macrocycle in turn modulate the chemical and photophysical properties of the biological chromophores. The axial ligand affinity of heme in heme proteins,<sup>4</sup> axial ligation and redox properties of cofactor F430 in methylreductase,<sup>5</sup> Co–C bond cleavage in coenzyme B<sub>12</sub>,<sup>6</sup> and the photosynthetic properties of light-gathering and energy-transducing systems in green plants<sup>7a</sup> and bacteria<sup>7b</sup> depend on the degree of flexibility and nonplanarity of the tetrapyrrole macrocycle.

The effects of nonplanarity on the properties of the porphyrin macrocycle have been explored using highly substituted porphyrins as nonplanar model compounds.<sup>8–15</sup> Variable-temperature NMR and resonance Raman studies have shown that the nonplanar conformation in crystals is retained in solutions. Nonplanar porphyrins show different oxidation potentials, red-shifted optical spectra, and different spin delocalizations compared to those of planar porphyrins. The axial ligand affinity is lower for nonplanar porphyrins than for the planar porphyrins.

Other studies have also correlated nonplanarity with axial ligand affinity. In series of  $\beta$ -oxoporphyrins and other reduced porphyrins found in F430, the flexibility of a nickel porphyrinic ring enhances axial ligand binding.<sup>5b,16</sup> The more distorted the tetrapyrrole ring, the more flexible it is, and this results in the higher axial ligand affinity. This is contradictory to the findings for normal porphyrins. However, different mechanisms appear to apply on the basis of the type of saturation of the tetrapyrrole

\* Author to whom correspondence should be addressed.

† Middlebury College.

‡ University of California.

• Abstract published in *Advance ACS Abstracts*, August 1, 1994.

- (1) Dolphin, D. *The Porphyrins*; Academic Press: New York, 1978.
- (2) Dolphin, D. *Biomimetic Chemistry*; American Chemical Society: Washington, DC, 1980.
- (3) (a) Hoard, J. L. In *Porphyrins and Metalloporphyrins*; Smith, K. M., Ed.; Elsevier: Amsterdam, 1975; Chapter 8. (b) Scheidt, W. R. In *The Porphyrins*; Academic Press: New York, 1979; Vol. 3, Chapter 10. (c) Scheidt, W. R.; Lee, Y. J. *Struct. Bonding (Berlin)* **1987**, *64*, 1–11.
- (4) Alden, R. G.; Ondrias, M. R.; Shelnut, J. A. *J. Am. Chem. Soc.* **1990**, *112*, 691–697.
- (5) (a) Pfaltz, A. In *The Bioinorganic Chemistry of Nickel*; Lancaster, J. R., Ed.; VCH Publishers: New York, 1988; Chapter 12. (b) Eschenmoser, A. *Ann. N.Y. Acad. Sci.* **1986**, *471*, 106–123. (c) Juan, B.; Pfaltz, A. *J. Chem. Soc., Chem. Commun.* **1986**, 1327–1329. (d) Furenliid, L. R.; Renner, M. W.; Fajer, J. *J. Am. Chem. Soc.* **1990**, *112*, 8987–8989.
- (6) (a) Geno, M. K.; Halpern, J. *J. Am. Chem. Soc.* **1987**, *109*, 1238–1240. (b) Babier, B. M. In *B<sub>12</sub>*; Dolphin, D., Ed.; Wiley: New York, 1982; Vol. 2, Chapter 10.
- (7) (a) Deisenhofer, J.; Michel, H. *Science* **1989**, *245*, 1463–1473. (b) Trounoud, D. E.; Schmid, M. F.; Mathews, B. W. *J. Mol. Biol.* **1986**, *188*, 443–454.

- (8) Barkigia, K. M.; Chantranpong, L.; Smith, K. M.; Fajer, J. *J. Am. Chem. Soc.* **1988**, *110*, 7566–7567.
- (9) Barkigia, K. M.; Berber, M. D.; Fajer, J.; Medforth, C. J.; Renner, M. W.; Smith, K. M. *J. Am. Chem. Soc.* **1990**, *112*, 8851–8857.
- (10) Renner, M. W.; Cheng, R. J.; Chang, C. K.; Fajer, J. *J. Phys. Chem.* **1990**, *94*, 8508–8511.
- (11) (a) Medforth, C. J.; Berber, M. D.; Smith, K. M. *Tetrahedron Lett.* **1990**, *31*, 3719–3722. (b) Medforth, C. J.; Smith, K. M. *Tetrahedron Lett.* **1990**, *31*, 5583–5586.
- (12) Shelnut, J. A.; Medforth, C. J.; Berber, M. D.; Barkigia, K. M.; Smith, K. M. *J. Am. Chem. Soc.* **1991**, *113*, 4077–4087.
- (13) Medforth, C. J.; Senge, M. O.; Smith, K. M.; Sparks, L. D.; Shelnut, J. A. *J. Am. Chem. Soc.* **1992**, *114*, 9859–9869.
- (14) Shelnut, J. A.; Majumder, S. A.; Sparks, L. D.; Hobbs, J. D.; Medforth, C. J.; Senge, M. O.; Smith, K. M.; Miura, M.; Luo, L.; Quirke, J. M. E. *J. Raman Spectrosc.* **1992**, *23*, 523–529.
- (15) Sparks, L. D.; Medforth, C. J.; Park, M.-S.; Chamberlain, J. R.; Ondrias, M. R.; Senge, M. O.; Smith, K. M.; Shelnut, J. A. *J. Am. Chem. Soc.* **1993**, *115*, 581–592.
- (16) (a) Connick, P. A.; Macor, K. A. *Inorg. Chem.* **1991**, *30*, 4654–4663. (b) Connick, P. A.; Haller, K. J.; Macor, K. A. *Inorg. Chem.*, in press.

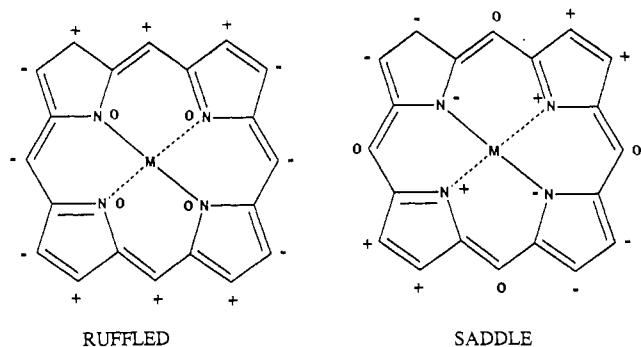


**Figure 1.** Idealized ruffled and saddle distortion modes for the porphyrin macrocycle. Displacements of the atoms with respect to the porphyrin least-squares plane are shown as + = above the plane, - = below the plane, and 0 = in the plane.<sup>14</sup>

ring and/or on the type of nonplanarity. Crystal structures of the corphin<sup>17</sup> and corrin rings<sup>18</sup> show them to be considerably more ruffled than the porphyrin rings,<sup>19</sup> and the molecular orbital energy level diagrams for porphyrins<sup>15</sup> and reduced porphyrins<sup>16a</sup> are different.

Recently dodecasybstituted porphyrins with macrocycles which distort from planarity in different ways were prepared.<sup>13</sup> They are classified into two major classes; one has four meso alkyl groups favoring a ruffled conformation and the other has four meso phenyl groups favoring a saddle conformation (Figure 1). The optical spectra for these compounds are shifted to lower energy compared to those for planar porphyrins. However, the magnitudes of the shifts in the absorption spectra are quite different. Different types and different degrees of distortion, as well as different electron-donating substituents, may all contribute to the shifts. INDO/CI calculations show that both the macrocycle conformation and the peripheral substituents affect the optical absorption spectra.<sup>15</sup>

The purpose of this study is to detect the influence of different types of nonplanarity on the electronic structure of porphyrins by MCD spectroscopy. Theoretical calculations have predicted that both the  $a_{1u}$  and  $a_{2u}$  orbitals are destabilized more than the  $e_g^*$  orbital as the macrocycle distorts, resulting in lower  $\pi \rightarrow \pi^*$  transition energy.<sup>12</sup> However, the reduction in symmetry associated with nonplanarity, which may affect the degeneracy of the excited state, has not been examined. Previous MCD studies have reported a splitting of the excited state degeneracy and sign inversion in the Q region (500–700 nm) of chlorins and asymmetrically substituted porphyrins due to a disruption of the local  $D_{4h}$  symmetry.<sup>20</sup> Therefore, it is plausible that a reduction in symmetry associated with conformational distortion could also produce characteristic signals in the MCD spectra.

Another purpose of this study is to find a way for judging the axial ligation state of nickel porphyrins by MCD. UV/vis, RR, and EPR spectroscopic studies have all been used to study the axial ligation state. Axial ligation lowers the energy of the porphyrin  $\pi \rightarrow \pi^*$  electronic transition, lowers the porphyrin ring vibrational energies, and changes the spin state from a singlet to a triplet. Therefore, it is not straightforward to differentiate

the 5-coordinate species from the 6-coordinate species by these methods. The relative intensity of the Soret (350–500 nm) and the Q MCD bands differs depending on the coordination state.<sup>21</sup> By comparison of the intensities of these bands of nickel porphyrins whose coordination number is known, we may find a way of differentiating 4-, 5-, and 6-coordinate species.

With these objectives in mind, we have studied the MCD spectra of nickel(II) octaethylporphyrin (NiOEP) (mixture of planar and ruffled porphyrin ring), nickel(II) tetracyclopentyltetrapentylporphyrin (NiTC<sub>5</sub>TC<sub>5</sub>P) (ruffled porphyrin ring induced by twisted pyrrole groups), nickel(II) octaethyltetraphenylporphyrin (NiOETPP) (saddle-shaped porphyrin ring induced by tilted pyrrole groups) (Figure 2), and Ni(II)-reconstituted hemoglobin (NiHb) and myoglobin (NiMb).

## Experimental Section

**Materials.** NiOEP and NiPP were obtained from Mid-Century Chemicals (Posen, IL) and used without further purification. NiTC<sub>5</sub>TC<sub>5</sub>P and NiOETPP were prepared using the procedure described previously.<sup>13</sup> Spectrophotometric grade ether, pyrrolidine, and glycerol were obtained from Aldrich (Milwaukee, WI), NiHb was kindly supplied by Dr. J. A. Shelnett, and NiMb was prepared by the method of Alston and Storm.<sup>22</sup>

**Sample Preparation.** Samples for room-temperature studies were dissolved in solvent at the concentration ( $\sim 10^{-6}$ – $10^{-5}$  M) which gave an absorbance of about 1 at the Soret band maxima in a 1-cm cell. Ligand affinity studies were run in neat pyrrolidine. Low-temperature studies were run in pyrrolidine/glycerol (3/1, v/v) to produce a transparent glass.

**Data Collection.** UV/vis spectra were collected on a Cary 17 spectrophotometer, interfaced with a computer using version 8.04 software by OLIS (Jefferson, GA). MCD spectra were recorded on a Jasco J-600 spectropolarimeter equipped with 1.4-T electromagnet (1.4 T) as well as a superconducting magnet (Oxford Instruments, Oxford, U.K.) generating magnetic fields to 4.0 T, in the temperature range 1.5–300 K.

## Results and Discussion

Figures 3–5 show the MCD and UV/vis spectra of NiOEP, NiTC<sub>5</sub>TC<sub>5</sub>P, and NiOETPP in ether at room temperature. There is an increase in the wavelength of the  $\pi \rightarrow \pi^*$  transitions (Soret and Q bands) in the order OEP < TC<sub>5</sub>TC<sub>5</sub>P < OETPP. Theoretical calculations<sup>15</sup> show that this red shift is due to the destabilized porphyrin  $\pi$  orbitals. Both the  $a_{1u}$  and  $a_{2u}$  orbitals are destabilized more than the  $e_g^*$  orbital, so that the separation between the HOMO (highest occupied molecular orbital) and LUMO (lowest unoccupied molecular orbital) is smaller for the nonplanar conformation.<sup>23</sup> The red shift suggests an increase in nonplanarity. However, the electron-withdrawing capacity of the phenyl group may also contribute to the larger red shift in the absorption spectrum of NiOETPP.<sup>15</sup>

The MCD spectra of all three species, NiOEP, NiTC<sub>5</sub>TC<sub>5</sub>P, and NiOETPP in ether, consist of derivative-shaped curves with a crossover (zero) point at the zero-field absorption maxima. There are three types of terms that can contribute to MCD spectral intensity: *A*-term, *B*-term, and *C*-term.<sup>20,24</sup> The *A*-term arises from transitions involving degenerate initial or final states. *A*-term MCD band shape resembles the derivative of the absorption spectrum. When the low-energy (long-wavelength) side of the

(17) (a) Pfaltz, A.; Juan, B.; Fassler, A.; Eschenmoser, A.; Jaenchen, R.; Gilles, H. H.; Diekert, G.; Thauer, R. K. *Helv. Chim. Acta* **1982**, *65*, 828–832. (b) Kratky, C.; Waditschatka, R.; Angst, C.; Johansen, J. E.; Plaquent, J. C.; Schreiber, J.; Eschenmoser, A. *Helv. Chim. Acta* **1985**, *68*, 1312–1337.  
 (18) Glusker, J. In *B<sub>12</sub>*; Dolphin, D., Ed.; Wiley: New York, 1982; Vol. 1, Chapter 3.  
 (19) (a) Kendrew, J. C.; Dickerson, R. E.; Strandberg, B. E.; Hart, R. G.; Davies, D. R.; Phillips, D. C.; Shore, V. C. *Nature* **1960**, *185*, 422–426. (b) Muirhead, H.; Greer, J. *Nature* **1970**, *228*, 516–519. (c) Scheidt, W. R.; Lee, Y. J. *Struct. Bonding (Berlin)* **1987**, *64*, 1–70.  
 (20) (a) Michl, J. *J. Am. Chem. Soc.* **1978**, *100*, 6801–6819. (b) Keegan, J. D.; Stolzenberg, A. M.; Lu, Y.-C.; Linder, R. E.; Barth, G.; Moscovitz, A.; Bunnenberg, E.; Djerassi, C. *J. Am. Chem. Soc.* **1982**, *104*, 4305–4329. (c) Goldbeck, R. A. *Acc. Chem. Res.* **1988**, *21*, 95–101.

(21) Ceulemans, A.; Oldenhof, W.; Gorller-Walrand, C.; Vanquickenborne, L. G. *J. Am. Chem. Soc.* **1986**, *108*, 1155–1163.  
 (22) Alston, K.; Storm, C. B. *Biochemistry* **1979**, *18*, 4292–4299.  
 (23) Alden, R. G.; Crawford, B. A.; Doolen, R.; Ondrias, M. R.; Shelnett, J. A. *J. Am. Chem. Soc.* **1989**, *111*, 2070–2072.  
 (24) (a) Sutherland, J. C. In *The Porphyrins*; Dolphin, D., Ed.; Academic Press: New York, 1978; Vol. III, pp 225–248. (b) Holmquist, B. In *The Porphyrins*; Dolphin, D., Ed.; Academic Press: New York, 1978; Vol. III, pp 249–270. (c) Sutherland, J. C.; Holmquist, B. *Annu. Rev. Biophys.* **1980**, *9*, 293. (d) Dawson, J. H.; Dooley, D. M. In *Fe Porphyrins*; Lever, A. B. P., and Gray, H. B., Eds.; VCH: New York, 1989; Part 3, Chapter 1. (e) Johnson, M. K. In *Physical Methods in Inorganic and Bioinorganic Chemistry*; Que, L., Ed.; University Science Books: Milwaukee, WI, 1993.

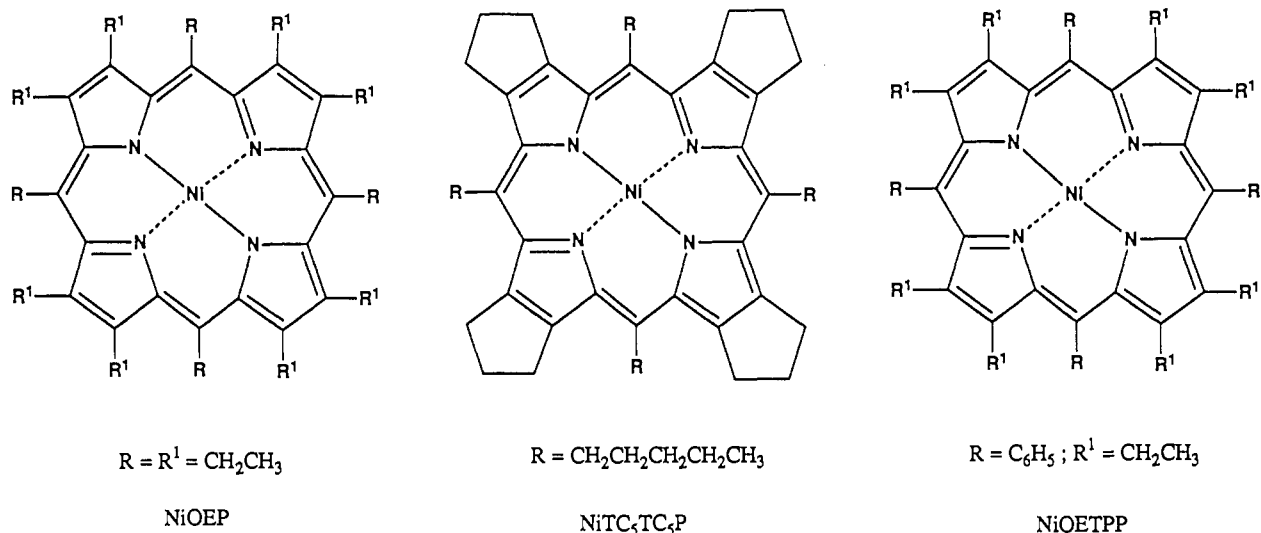


Figure 2. Molecular structures of NiOEP, NiTC<sub>5</sub>TC<sub>5</sub>P, and NiOETPP.<sup>14</sup>

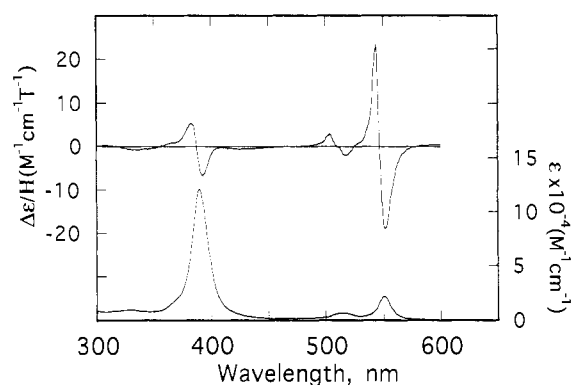


Figure 3. MCD and UV/vis spectra of NiOEP in ether recorded at room temperature, with a magnetic field of 1.4 T.

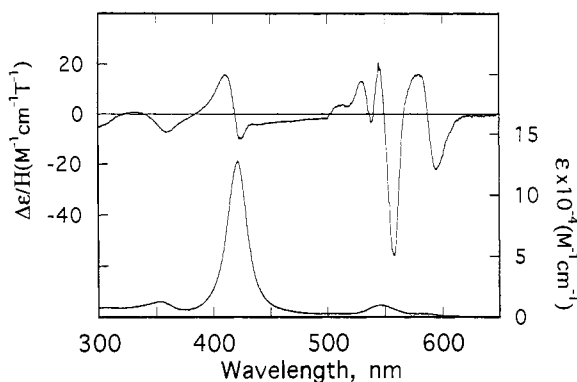


Figure 4. MCD and UV/vis spectra of spectra of NiTC<sub>5</sub>TC<sub>5</sub>P in ether recorded at room temperature, with a magnetic field of 1.4 T.

band shows negative ellipticity and the high-energy side shows positive ellipticity, it is called a positive or "normal" *A*-term. A crossover (zero) point of the derivative-shaped curve of a "normal" *A* term is at the zero-field absorption maximum. *B*-term MCD arises from magnetically induced mixing of any states. The *B*-term line shape is the same as the line shape of the corresponding absorption band. *C*-term MCD arises from transitions from a degenerate ground state and is temperature dependent. The MCD spectra of metalloporphyrins with no unpaired electrons, such as nickel(II) porphyrins, are characterized by *A*-term and/or *B*-term MCD.

The MCD spectra of all three compounds at low temperature (down to 2 K, spectra not shown) are essentially the same as those at room temperature, except for slightly different peak wavelengths due to changes in the vibronic envelope with temperature. Therefore, the MCD spectral features of all the

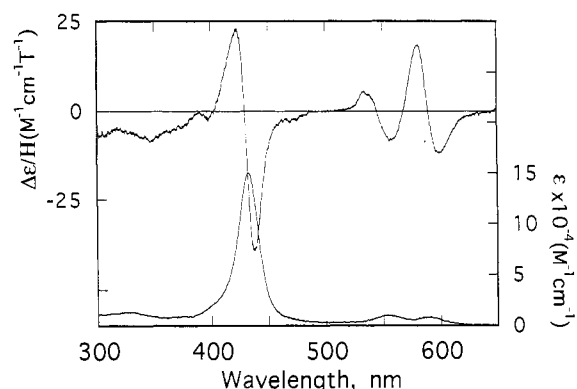


Figure 5. MCD and UV/vis spectra of spectra of NiOETPP in ether recorded at room temperature, with a magnetic field of 1.4 T.

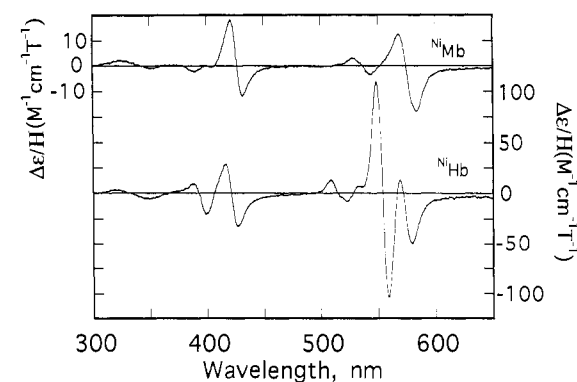
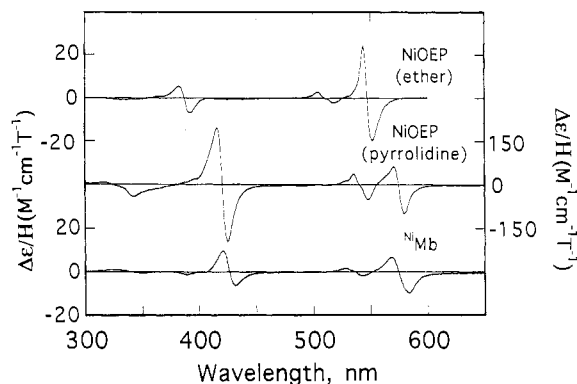


Figure 6. MCD spectra of <sup>Ni</sup>Mb and <sup>Ni</sup>Hb in 0.1 M phosphate buffer (pH 7.4) recorded at room temperature, with a magnetic field of 1.4 T.

three compounds can be characterized by "normal" *A*-term MCD peaks in the Soret and Q regions. This means that the excited state degeneracies of all three compounds are retained. It is noted that there is a large difference between the shapes of the left and right wings of the *A*-term in the Soret region of NiTC<sub>5</sub>TC<sub>5</sub>P in ether (Figure 4). This band asymmetry is attributed to an underlying *B*-term arising from the magnetically induced mixing of B (Soret) and Q states.<sup>21</sup> Therefore, it is concluded that the excited state degeneracies are not lifted to an extent greater than the transition bandwidths, and the *D*<sub>2d</sub> symmetry in both cases is approximately retained.

Figure 6 shows the MCD spectra of <sup>Ni</sup>Mb and <sup>Ni</sup>Hb at room temperature. Their low-temperature (down to 2 K) MCD spectra (not shown) are essentially the same as those at room temperature. The MCD peaks are all "normal" *A*-terms, which is consistent



**Figure 7.** MCD spectra of NiOEP in ether, NiOEP in pyrrolidine, and  $\text{Ni}^{\text{Mb}}$  recorded at room temperature, with a magnetic field of 1.4 T.

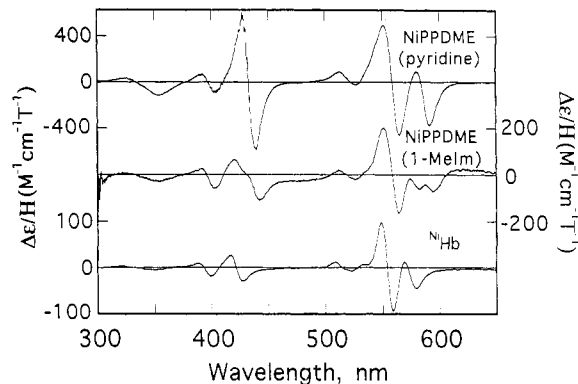
**Table 1.** Ratios of the Soret MCD Band Intensities to the Q MCD Band Intensities ( $I_S/I_Q$ ) in Several Nickel Porphyrins in Various Coordinating and Noncoordinating Solvents.

	solvent	coordn no.	$I_S/I_Q$
NiOEP	ether	4	0.27
	pyridine	4	0.28
	dichloromethane	4	0.30
	pyrrolidine	6	2.4
NiPPDME	ether	4	0.23
	pyridine	4	0.16
	pyrrolidine	6	2.5
	pyrrolidine	6	1.5
	1-methylimidazole	4	0.22
$\text{Ni}^{\text{Mb}}$	phosphate buffer	5	1.0
	$\text{Ni}^{\text{Hb}}$	4	0.17
$\text{NiTC}_5\text{TC}_3$	phosphate buffer	5	1.2
	pyrrolidine	6	3.3

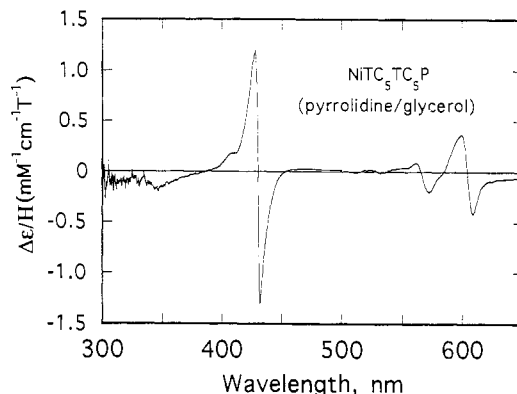
with the RR study showing that the protein environment forces the NiPP macrocycle into a planar conformation in hemoglobin.<sup>4</sup>

Figure 7 compares the MCD spectra of NiOEP in ether and pyrrolidine and  $\text{Ni}^{\text{Mb}}$  at room temperature. NiOEP in ether (4-coordinate) has a more intense Q band than Soret band. NiOEP in pyrrolidine (6-coordinate)<sup>12</sup> shows the normal MCD spectral features with a weaker Q peak relative to the Soret peak (opposite to the 4-coordinate species). In the MCD spectrum of  $\text{Ni}^{\text{Mb}}$  (5-coordinate NiPP<sup>25</sup>), the Soret and Q MCD band intensities are about the same. We measured the magnitude of the difference between  $\Delta\epsilon/H$  values of the peak and trough for both the Soret ( $I_S$ ) and Q ( $I_Q$ ) bands for various nickel porphyrins in various coordinating and noncoordinating solvents and calculated their ratio ( $I_S/I_Q$ ) (Table 1). For the compounds tested in this work,  $I_S/I_Q$  is  $\sim 0.2$ – $0.3$  for 4-coordinate,  $\sim 1$  for 5-coordinate, and  $\sim 2$ – $3$  for 6-coordinate species.

This trend for nickel porphyrins may be useful for identifying the coordination states of nickel porphyrins. Figure 8 shows the MCD spectra of Ni(II) species with mixed coordination numbers: NiPPDME (nickel(II) protoporphyrin IX dimethyl ester) in pyridine, NiPPDME in 1-methylimidazole, and  $\text{Ni}^{\text{Hb}}$ . The MCD spectrum of NiPPDME in pyridine consists of a pair of weaker Soret/stronger Q ( $I_S/I_Q = 0.16$ ) and stronger Soret/weaker Q bands ( $I_S/I_Q = 2.5$ ), suggesting a mixture of 4- and 6-coordinate species. The MCD spectrum of NiPPDME in 1-methylimidazole also consists of a pair of weaker Soret/stronger Q ( $I_S/I_Q = 0.22$ ) and stronger Soret/weaker Q bands ( $I_S/I_Q = 3.2$ ), suggesting a 4- and 6-coordinate mixture. The MCD spectrum of  $\text{Ni}^{\text{Hb}}$  consists of a pair of weaker Soret/stronger Q ( $I_S/I_Q = 0.17$ ) and medium Soret/medium Q bands ( $I_S/I_Q = 1.2$ ), suggesting a mixture of 4- and 5-coordinate species. These are consistent with the results of the RR study.<sup>25</sup>



**Figure 8.** MCD spectra of NiPPDME in pyridine, NiPPDME in 1-methylimidazole (1-Melm), and  $\text{Ni}^{\text{Hb}}$  recorded at room temperature, with a magnetic field of 1.4 T.



**Figure 9.** MCD spectrum of  $\text{NiTC}_5\text{TC}_3\text{P}$  in pyrrolidine/glycerol (3/1, v/v) recorded at 100 K, with a magnetic field of 4.0 T.

The affinity of NiPP in  $\text{Ni}^{\text{Hb}}$  or  $\text{Ni}^{\text{Mb}}$  for exogenous ligands such as 1-methylimidazole, cyanide, azide, and fluoride was monitored by MCD. No spectral changes were observed when these anions were added in a 100-fold excess even at 2 K.

Figure 9 shows the MCD spectrum of  $\text{NiTC}_5\text{TC}_3\text{P}$  in a pyrrolidine/glycerol (3/1, v/v) mixture at 100 K.  $I_S/I_Q$  is 3.3, suggesting that pyrrolidine has bound to  $\text{NiTC}_5\text{TC}_3\text{P}$  biaxially at 100 K. Binding of a  $\sigma$ -donating axial ligand raises the energy of the doubly occupied  $d_{z^2}$  orbital relative to its energy for the unligated nickel porphyrin, resulting in promotion of one electron to the unoccupied  $d_{x^2-y^2}$  orbital and a change in spin from a singlet ( $S = 0$ ) to a triplet ( $S = 1$ ) state.<sup>12</sup> The population of the antibonding  $d_{x^2-y^2}$  orbital results in a larger core,<sup>12</sup> which may relieve the porphyrin macrocycle deformation. At room temperature, there is a weak A-term peak as a shoulder on the red side of the Soret region of the noncoordinated  $\text{NiTC}_5\text{TC}_3\text{P}$  (spectrum not shown), indicating a small amount of an axially coordinated species. The driving force for the axial coordination at low temperature may be due to thermodynamic factors because the entropy change for axial ligation is negative. NiOETPP does not show any sign of axial coordination down to 100 K. Steric hindrance exerted by bulky phenyl groups may prohibit the axial ligation.

**Acknowledgment.** We are grateful to Dr. Kathleen A. Macor for critical reading of the manuscript and helpful discussions. Work performed at Middlebury College was supported by the Petroleum Research Fund. Acknowledgment is made to the donors of the Petroleum Research Fund, administered by the American Chemical Society (Grant ACS-PRF 24270-B3), for support of this research. Work at the University of California was supported by National Science Foundation Grant CHE-93-05577 (K.M.S.). C.J.M. gratefully acknowledges a Fulbright Travel Scholarship and an Associated Western Universities Postdoctoral Fellowship.

(25) Shelnutz, J. A.; Alston, K.; Ho, J.-Y.; Yu, N.-T.; Yamamoto, T.; Rifkind, J. M. *Biochemistry* 1986, 25, 620–627.